

Automated SpectroPhotometric Image REDuction (ASPIRED) – A PYTHON-based spectral data reduction toolkit

Marco C. Lam,^{1,2,3}   Robert J. Smith,²  Iair Arcavi,^{1,4}  Iain A. Steele,² 

Josh Veitch-Michaelis,²  and Lukasz Wyrzykowski³ 

¹*School of Physics and Astronomy, Tel Aviv University, Tel Aviv 69978, Israel*

²*Astrophysics Research Institute, Liverpool John Moores University, IC2, LSP, 146 Brownlow Hill, Liverpool L3 5RF, UK*

³*Astronomical Observatory, University of Warsaw, Al. Ujazdowskie 4, 00-478, Warszawa, Poland*

⁴*CIFAR Azrieli Global Scholars program, CIFAR, Toronto, Canada*

Accepted. Received; in original from

ABSTRACT

We provide a suite of publicly available spectral data reduction software to facilitate rapid scientific products from time-domain observations. The Automated SpectroPhotometric REDuction (ASPIRED) toolkit is aimed to be as general as possible with high flexibility such that it can work with different instruments. The default settings support typical low-resolution long-slit spectrometer configurations, whilst it also offers a flexible set of functions for users to refine and tailor-make automated pipelines to an instrument’s individual characteristics. Automation can provide immediate data reduction to allow adaptive observing strategies, which is particularly important in Time Domain Astronomy. ASPIRED is entirely PYTHON-based and is independent of IRAF.

Key words: software: development – software: public release

1 INTRODUCTION

With major global investments in multi-wavelength and multi-messenger surveys, time-domain astronomy is entering a golden age. In order to maximally exploit discoveries from these facilities, rapid spectroscopic follow-up observations of transient objects (e.g., supernovae, gravitational-wave optical counterparts etc.) is needed to provide crucial *astrophysical* interpretations. Part of the former OPTICON¹ project coordinates the operation of a network of largely self-funded European robotic and conventional telescopes, coordinating common science goals and providing the tools to deliver science-ready photometric and spectroscopic data in near real-time. The goal is to facilitate automated or interactive decision making, allowing "on-the-fly" modification of observing strategies and rapid triggering of other facilities. As part of the network’s activity, a software development work package was commissioned under the working title of Automated SpectroPhotometric REDuction (ASPIRED) toolkit, coordinated on Github².

The "industrial standard" of spectral and image reduction is of no doubt the IRAF software (Tody 1986, 1993). It has powered many reduction engines in the past and present. However, unfortunately, the software has reached the end-of-support state where there will no longer be any official support to the software, and it relies entirely on community support³.

In this generation of user-side Astronomy data handling and processing, as well as the emphasis in computing courses for scientists, PYTHON is among the most popular languages due to its ease to use with a shallow learning curve, readable syntax and simple way to "glue" different pieces of software together. Its flexibility to serve as a scripting and an object-oriented language makes it useful in many use cases: demonstrating with visual tools with little overhead, prototyping, web-serving, and it can be compiled if wanted. This broad range of functionality and high-level usage make it relatively inefficient. However, PYTHON is an excellent choice of language to build wrappers over highly efficient and well-established codes. In fact, some of the most used packages, SCIPY (Virtanen et al. 2020) and NUMPY (Harris et al. 2020), are written in FORTRAN and C respectively. Multi-threading and multi-processing are also possible with built-in and other third-party packages, e.g. MPI4PY (Dalcin et al. 2011).

Various efforts are being made to develop software for current and next-generation spectral data reduction. For example, PYPEIT (Prochaska et al. 2020a; Prochaska et al. 2020b) is designed for tailor-made reductions of various instruments, PYREDUCE (Piskunov et al. 2021) is designed for optimal Echelle spectral reduction (but does not handle sky subtraction); in the ASTROPY ‘Universe’ (Astropy Collaboration et al. 2013, 2018), SPECREDUCE is likely to be the next-generation user-focused data reduction package, but it is far from the stage of deployment at the time of writing. PYDIS has all the essential ingredients for reducing spectra but has been out of maintenance since 2016, and SPECUTILS handles spectral analysis and manipulation but not the reduction itself.

In ASPIRED, we have a different vision in how and what should be

* E-mail: lam@tau.ac.il

¹ <https://www.astro-opticon.org>; now the OPTICON-RadioNet Pilot <https://www.orp-h2020.eu>

² <https://github.com/cylammarco/ASPIRED>

³ <https://iraf-community.github.io>

abstracted from the users. Instead of providing a ready-to-go ‘black box’ suited for a specific instrument or observations made in particular conditions, we provide a toolkit that is as general as possible for users to have a set of high-level data reduction building blocks to process the data in the ways most appropriate to their instruments and observations. This shifts more of the work and maintenance to the user-end, but it will allow rapid modification of the data reduction workflow if there are any changes in the instrumental configuration, for example, a detector is refitted, and the detector plane is shifted and rotated by a few pixels. ASPIRED also aims to provide a set of functions that requires coding skills that students should have attained from university-level of Observational Astrophysics course.

We use the SPRAT family as our ‘first-light’ instruments for development (Piascik et al. 2014), but we aim to allow high-level tools for users to build and fine-tune their pipelines to support a wide range of configurations (Lam et al. 2020a; Lam 2021). As of the time of writing, we have successfully used ASPIRED to reduce data from the William Herschel Telescope *Intermediate-dispersion Spectrograph and Imaging System*⁴ (WHT/ISIS), Las Cumbres Observatory FLOYDS (Brown et al. 2013, LCO/FLOYDS), Gemini Observatory *Gemini Multi-Object Spectrographs* long slit mode (Hook et al. 2004, Gemini/GMOS-LS), Gran Telescopio Canarias *Optical System for Imaging and low-Intermediate-Resolution Integrated Spectroscopy* (Cepa et al. 2000, GTC/OSIRIS), and Telescopio Nazionale Galileo *Device Optimised for the LOW RESolution*⁵ (TNG/DOLORES); all of these are currently still unofficial sets of reduction procedures. The examples of these deployments can be found at <https://github.com/cylamarco/aspired-example>.

This paper is organised as follows: Section §2 covers the software’s development and organisation. Then, we go through the details of the spectral reduction procedures in Section §3. In the last section, we provide various links for references and instructions for installation.

This article is not intended to serve as an API document, nor as a review of the various methods concerning spectral extraction. Only the high-level descriptions and the scientific and mathematical technicalities that are important to the data reduction processes are discussed here.

2 DEVELOPMENT AND STRUCTURE OF ASPIRED

One of the development goals of ASPIRED is to design a piece of software that is as modular and portable as possible. We rely on as few external dependencies as possible. The ones we do use are those that would require a substantial programming effort to reproduce and have a proven track record of reliability and/or plan to remain maintained in the foreseeable future. The explicit top-level dependencies are – ASTROCRAPPY (McCully et al. 2018; van Dokkum 2001) ASTROPY (Astropy Collaboration et al. 2013, 2018), CCDPROC (Craig et al. 2017), NUMPY (Harris et al. 2020) PLOTLY (Plotly Technologies Inc. 2015), SCIPY (Virtanen et al. 2020) SPECTRES (Carnall 2017), and STATSMODELS (Seabold & Perktold 2010).

We host our source code on Github, which provides version control and other utilities to facilitate the development. It uses GIT⁶, issue and bug tracking, high-level project management, automation with GITHUB ACTIONS upon each commit for:

⁴ <https://www.ing.iac.es/astronomy/instruments/isis>

⁵ <http://www.tng.iac.es/instruments/lrs>

⁶ <https://git-scm.com>

(i) Continuous Integration (CI) to install the software in LINUX, MAC and WINDOWS system, and then perform unit tests with PYTEST (Krekel et al. 2004),

(ii) generating test coverage report with COVERALLS⁷ which identifies lines in the script that are missed from the tests,

(iii) Continuous Deployment (CD) through PYPPI⁸ that allows immediate availability of the latest numbered version,

(iv) dependency version tracking with DEPENDABOT⁹, and

(v) generating API documentation powered by SPHINX¹⁰ hosted on Read the Docs¹¹.

The initial work package divided the project broadly into three high-level independent components:

Graphical User Interface (not in active development)

In the beginning, we commissioned a prototype of the graphical user interface¹² ELECTRON¹³, which wraps on top of ASPIRED without needing to adapt the code. This is possible for a few reasons: first, PYTHON is an interpreter, it can execute in run time - it is straightforward to run itself as a server to handle the response from ELECTRON; second, there are many plotting libraries available, and there is not a unified API standard for creating a figure. It is difficult to maintain multiple plotting libraries to optimise certain plots for diagnostics and visualisations; PLOTLY¹⁴ has a good balance generating interactive and static plots, so it is chosen as our plotting engine; third, there is a JAVASCRIPT version of SAOIMAGES9¹⁵ that allows rapid and easy interactive image manipulation in a familiar fashion (Mandel & Vihkilin 2021). Given how ELECTRON and JS9 work like a web service, this prototype also shows that it can be deployed as an online tool. Such high-level of interactivity is, however, no longer in active development and currently only serves as a technology demonstrator of its capability.

Wavelength Calibration (not part of this work)

The wavelength calibration module is powered by the RANSAC Assisted Spectral CALibration (RASCAL, Veitch-Michaelis & Lam 2020a,b, Veitch-Michaelis & Lam in prep.), a software package developed in conjunction but independently of ASPIRED. It is improved on the work by Song et al. (2018), which searches only for *plausible* sets of arc lines that follow good linear approximations to the system. RASCAL considers the top N sets simultaneously. For each peak (pixel), the most common best-fit atlas line (wavelength) is chosen from the top candidate sets. This acts like a piece-wise linear fit and allows us to extract most of the correct matches from both the red and blue ends of the spectrum. RANdom SAMple Consensus (RANSAC, Fischler & Bolles 1981) is used to robustly fit a higher-order polynomial model to the candidate correspondences. The user is only required to supply a list of calibration lines (pixels), a list of peaks (wavelengths), and some knowledge (e.g. dispersion

⁷ <https://coveralls.io/github/cylamarco/ASPIRED>

⁸ <https://pypi.org/project/aspired>

⁹ <https://dependabot.com>

¹⁰ <https://www.sphinx-doc.org/en/master>

¹¹ <https://aspired.readthedocs.io/en/latest>

¹² <https://github.com/cylamarco/gASPIRED>

¹³ <https://www.electronjs.org>

¹⁴ <https://plotly.com>

¹⁵ <https://sites.google.com/cfa.harvard.edu/saoimages9>

resolution) of the system to initialise a most appropriate and efficient calibrator object for fitting the pixel-to-wavelength solution.

The Rest of the Spectral Extraction and Calibrations (this work)

This is the core of the ASPIRED, which mainly handles the spectral extraction and calibration processes. The software is organised into 3 main parts – `image_reduction`, `spectral_reduction`, and `spectrum1D`. The first two are the "overlords" that handle all the dependent classes and functions to orchestrate the operations. The third is a data structure that stores the metadata and the extracted data. The FITS file I/O handling is also handled by `spectrum1D`.

2.1 Data Reduction Modules

2.1.1 `image_reduction`

This module allows combining, subtracting and dividing of light, dark, bias and flat frames. The FITS header of the first light frame provided is copied over, while the headers from the other frames are not stored – only the file paths are stored as meta-data. The image reduction meta-data are appended to the end of the FITS header. Depending on the convention adopted by the observatories, the FITS file is defaulted to contain an empty `PrimaryHDU` with the process data stored in the first `ImageHDU` extension as recommended in the FITS Standard document¹⁶, or it can be stored directly in the `PrimaryHDU` as most users tend to opt for. Many forms of interactive and static images can be exported, powered by the `PLOTLY` image renderer.

ASPIRED intends to provide basic image reduction methods, sufficient for simple optical systems, which are the primary targets of ASPIRED. For example, a long slit spectrograph with a rectilinear 2D spectrum illuminated on the detector plane, i.e. the dispersion and spatial directions are perfectly perpendicular to each other across the entire detector plane. It is usually not immediately suitable for complex systems that have multiple non-parallel spectra illuminated on the detector plane. In the FLOYDS reduction example, we demonstrate how two non-parallel, highly curved spectra in a single 2D spectral image can be reduced and extracted by applying a mask to the data.

2.1.2 `spectral_reduction`

This is a large module that covers both 1D and 2D operations. In 2D, it provides image rectification, spectral tracing and spectral extraction. In 1D, it can perform wavelength calibration, flux calibration, atmospheric extinction correction and Telluric absorption correction. Diagnostic images can be exported at each step of operation, including the wavelength calibration that wraps around RASCAL and uses their native plotting capability. Outputs can be in FITS or ASCII files, e.g. CSV, where possible. See the next section for the mathematical and scientific descriptions of the various methods.

2.1.3 `spectrum1D`

This module provides a uniform format to store the metadata and the extracted data throughout the entire spectral extraction process. Data storage of observational data is almost exclusively done with FITS files, but they are not human readable. In view of that, ASPIRED

provides I/O handling of both FITS and ASCII-type files. All the higher-level functions are wrappers on top of a `spectrum1D` object.

3 SPECTRAL REDUCTION

In the highest-level terms, spectral reduction procedures after image reduction include: (1) identifying the spectrum/a, (2) tracing the spectrum/a, (3) correcting for image distortion, (4) extracting the spectrum/a, (5) performing wavelength calibration of the science target and a standard star, (6) computing the sensitivity curve using the standard observations, (7) performing atmospheric extinction correction, and finally (8) removing Telluric absorption. We omit a few common processes which we believe should be considered as part of the post-extraction processes or spectral analysis and manipulation. There are many sophisticated software packages with good and long track records to handle these processes post hoc. For example, sky glow subtraction with `SKYCORR` (Noll et al. 2014), or Telluric absorption removal **without** supplementary calibration data with `MOLEFIT` (Smette et al. 2015; Kausch et al. 2015). The following describes the technical details of the eight steps, where we use the following convention: the spectral image is dispersed on the detector plane such that the left side (small pixel number) corresponds to the blue part of the spectrum and the right side (large pixel number) to the red part.

3.1 Spectral Identification and Tracing

Conventionally, to obtain the position of a spectrum (i.e. trace), the centre of a spectrum in the dispersion direction is first identified, then a choice algorithm will scan across the spectral image to identify the spectral position over the entire dispersion direction. Instead, in ASPIRED, the `ap_trace()` function works by dividing the 2D spectrum into sub-spectra, and then each part is summed along the spectral direction before cross-correlating with the adjacent sub-spectra. This way, both the shift and the scaling of the spectrum/a along the spectral direction can be found simultaneously. The middle of the 2D spectrum is used as the zero point of the procedure. Here is a detailed description of the algorithm:

- (i) The input 2D spectrum is divided into `nwindow` sub-spectra.
- (ii) Each sub-spectrum is summed along the spectral direction in order to improve the signal(s) of the spectrum/a along the spatial direction – we call this a spatial spectrum.
- (iii) Each spatial spectrum is upsampled by a factor of `resample_factor` to allow for sub-pixel correlation precision. This utilises the `scipy.signal.resample()` function to fit the spatial profile with a spline.
- (iv) The *i*-th spatial spectrum is then cross-correlated to the *i*+1-th spatial spectrum. The shift and scale where the maximum occurs within the tolerance limit, `tol` is then stored.
- (v) The shifts relative to the central sub-spectrum are used to fit for a polynomial solution that defines the position of the trace.
- (vi) While the spatial spectra are cross-correlated, they are aligned and stacked for peak finding and Gaussian fitting towards the end of the iteration. Peak finding is performed with `scipy.signal.find_peaks()` and returns the list of peaks sorted by their prominence. Only centroiding has to be accurate at this stage, so a Gaussian function is sufficient. The standard deviation of the Gaussian is only served as a first guess of the profile when performing optimal extraction; it would not be used in the case of top-hat extraction (see section §3.3).

¹⁶ https://fits.gsfc.nasa.gov/fits_documentation.html

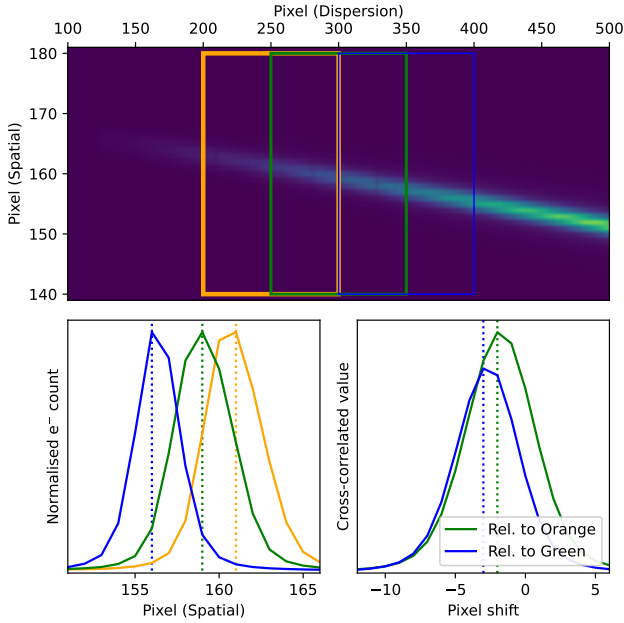


Figure 1. Top: A LT/SPRAT spectrum is rotated to illustrate how cross-correlation is used to find the shift between neighbouring sub-spectra. The orange, green and blue boxes are three example sub-spectra. Bottom left: the three sub-spectra are summed in the dispersion direction to generate the three profiles that are cross-correlated to compute the shift. Bottom right: the cross-correlated function for the green sub-spectrum relative to the orange sub-spectrum (plotted in green), and the one for the blue sub-spectrum relative to the green sub-spectrum (plotted in blue).

This procedure is illustrated in Fig. 1. Manually supplying a trace is possible with the `add_trace()` function. This is particularly useful for faint and/or confused sources that are beyond the capability of automated tracing. For example, if there is a faint transient source on top of a galaxy, a manual offset may be needed for extraction if the host is dominating the flux to a level that forced extraction is necessary. Otherwise, we recommend extracting the two (or more) most significant peaks for validation; the number needed depends on the environment and the morphology of the galaxy.

3.2 Image Rectification

In most cases, a spectrum on the detector plane is not only tilted, but it is also sufficiently distorted that the extraction has to be performed along a curve in order to perform sky subtraction properly. While this does not cause any complication in the tracing, the spatial and dispersion directions are no longer aligned with the x - y axes of the detector plane. `PyREDUCE` can optimally extract such highly distorted spectra, but the lack of sky subtraction using the "wings" in the sky region beyond the line-spread-profile has limited the usage in a typical single-frame extraction without an accompanying sky observation at an identical slit position. Alternatively to extracting along a curve, the 2D image can be rectified based on the spectral trace and sky emission or arc lines before extraction, so that the latter is performed on a spectrum (nearly) perfectly aligned with the detector x - y axes. Using the arc function for this process will deliver a more reliable rectification function.

The rectification in the spatial direction depends **only** on the trace. Each column of pixels gets (scaled and) shifted by resampling to

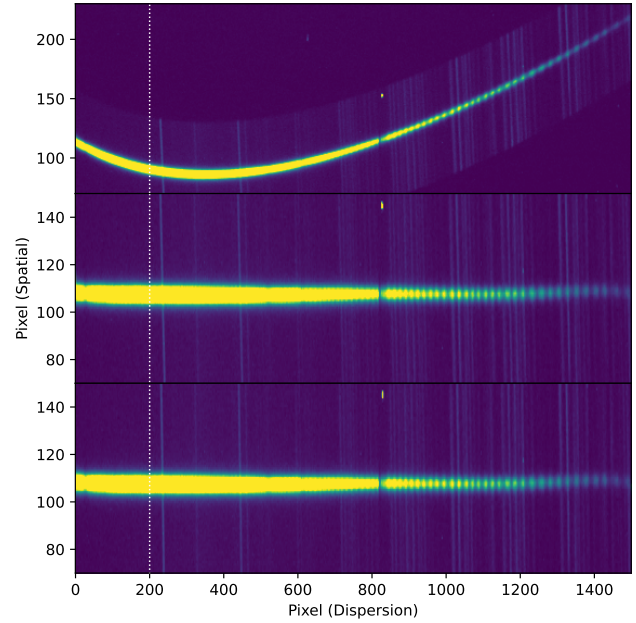


Figure 2. A 2D spectrum from LCO/FLOYDS is used to demonstrate the rectification procedure. The dotted white line is aligned in the spatial direction to serve as a visual guide. Top: The trimmed image of a FLOYDS spectrum. Middle: The 2D spectrum is resampled in the spatial direction based on the polynomial function of the trace. Bottom: The 2D spectrum is resampled in the dispersion direction. The shifts and scales are found by cross-correlating the sub-spectra divided in the spatial direction. This is perpendicular to the tracing process.

align with the centre of the spectrum. This will usually leave us with a spectrum tilted or curved in the dispersion direction. Therefore, the same procedure for tracing the spectra is applied in the spatial direction to find the best fit polynomial solution for shifting (and scaling) in the dispersion direction for the second step of the rectification process (See Fig. 2).

At the time of writing, this process is only possible if there is one trace. If more than one trace is found/provided, only the first one will get processed. The resampling is performed with `scipy.ndimage.zoom` which interpolates with a spline (the electron count is not always perfectly conserved, but the difference is negligible). It is possible to supply a set of pre-computed polynomials to perform the rectification, which can significantly speed up the data reduction process of a stable optical system.

3.3 Spectral Extraction

There are a few commonly used extraction methods; some work for all kinds of spectral images, some only work with specific observing strategies (e.g. the flat-relative optimal extraction; [Zechmeister et al. 2014](#)). The standard textbook method is commonly called the *top-hat* extraction or the *normal* extraction. It simply sums the electron counts over a given size of the aperture, and is robust and easy to use. However, this method does not deliver the maximal signal-to-noise ratio (SNR) from the available data. Various optimal extraction algorithms can increase the SNR. This works by down-weighting the wings of the spectral profile where almost all the photons are coming from the sky rather than the source (see Fig. 7). An optimal extraction can boost the SNR, particularly for background-limited sources,

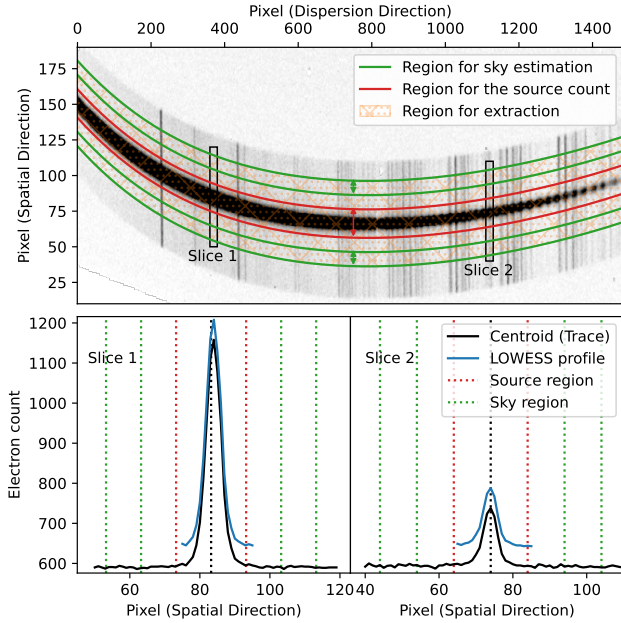


Figure 3. The same spectrum as in Figure 2 but the 2D spectral image is slightly rotated to have the sky lines aligned with the spatial direction with the y-axis. Top: The regions used for source and sky extractions are marked by the red and green lines and arrows. The light shade of orange hash marks denotes the entire region that is used for spectral extraction. The two boxes show the two columns of pixels fitted with profiles in the bottom half of the figure (the boxes are inflated for clarity). Bottom: The electron counts across the two slices, The vertical black dashed line is the centroid (trace) of the spectrum, the two red dashed lines mark the regions of the source and the pairs of green dashed lines on each side of the centroid are showing the regions used for sky extractions, respectively. The black line is the measured spectral profile (data), the blue line is the fitted LOWESS line-spread-function (model), offset for clarity.

which are the case in most observations (see Fig. 4). The extracted spectra and their associated uncertainties and sky background counts can be plotted for inspection. The residual image can also be exported for diagnostics.

Tophat/Normal Extraction

The top-hat extraction does not weigh the pixels for extraction, so every pixel has an equal contribution to the source count. Thus, it is very robust in getting the total electron count across a slice of pixels. The sky background count can be extracted from the regions outside the extraction aperture to be subtracted from the spectrum.

Horne-86 Optimal Extraction

[Horne \(1986, hereafter H86\)](#) is the golden standard of optimal extraction of spectra from modern electronic detectors. We follow the H86 recipe except for the profile modelling, where we provide three options: The first is a fixed Gaussian profile, the second uses LOcally Weighted Scatterplot Smoothing ([Cleveland 1979, LOWESS](#)) regression to fit for a polynomial, and the third accepts a manually supplied profile.

The default option is to use the LOWESS fit because it is the least sensitive to noise, cosmic ray contamination and detector artefacts.

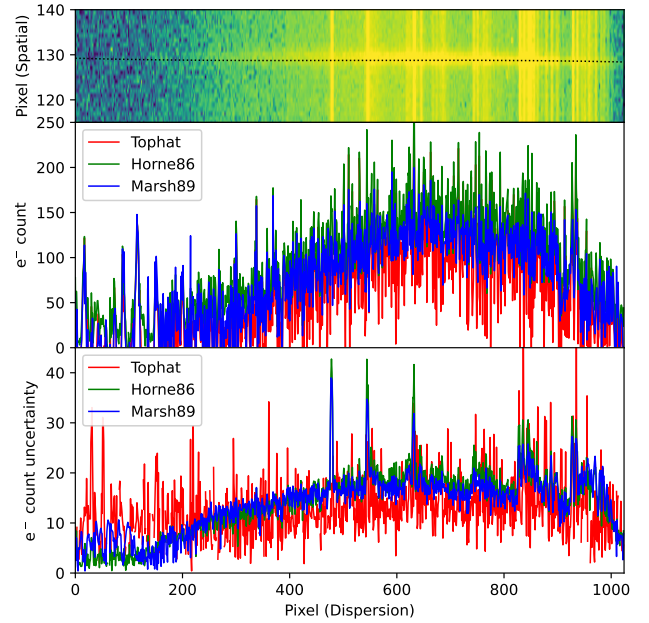


Figure 4. Top: An LT/SPRAT spectrum of a featureless ultra-cool white dwarf PSO J1801+625 ([Lam et al. 2020b](#)). Middle: The extracted spectra in electron counts using the three extraction methods are very similar. Bottom: The uncertainties with the three extraction methods in units of electron counts. The top-hat method is clearly noisier than the two optimal methods at the faint ends of the spectrum.

It is also flexible enough to allow a good fit for the profile of a resolved galaxy. This may, however, be less accurate for extracting a faint spectrum when the image is dominated by background noise. In such a case, the Gaussian profile is recommended as the profile is constructed from fitting the line-spread function from the total stack of all the sub-spectra (as described in Sec. 3.1). The quality of a valid profile should be as good as an extraction performed with the top-hat extraction method.

Marsh-89 Optimal Extraction

[Marsh \(1989, hereafter M89\)](#) improves on the H86 algorithm by fitting the change in the shape and centroid of the profile from one end of the spectrum to the other. It is very suited for extracting a highly tilted spectrum where the tilting direction is aligned with only **one** direction in the x - or the y -axis of the detector. Here we adapt Ian Crossfield’s set of public PYTHON 2 code for Astronomy^{17, 18} to PYTHON 3.

3.4 Wavelength Calibration

The wavelength calibration is powered by RASCAL, which is a concurrent development to this work. All the public functions from RASCAL are available in ASPIRED so users can have fine control over the calibration. The diagnostic plots are the set provided by RASCAL. They include the spectrum of the arc lamp where the traces on the science and standard frames are, which also shows where the

¹⁷ <https://people.ucsc.edu/~ianc/python/>

¹⁸ <https://crossfield.ku.edu/python/>

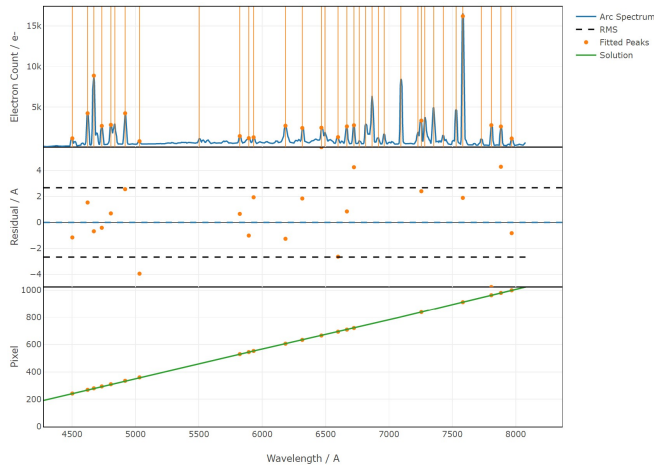


Figure 5. The wavelength calibration diagnostic plots from RASCAL. Top: the arc is plotted in blue, the fitted peaks are marked by the orange dots. Middle: The residual plot shows the difference between the fitted peaks and the true wavelengths. Bottom: The pixel-wavelength function (green) is over-plotted with the fitted peaks (orange).

peaks are detected; the peak-line pairs and the constrained space where the Hough-pairs are selected (see Veitch–Michaelis & Lam 2020b); and a plot showing the fitting solution and its quality (Fig. 5).

The polynomial coefficients for the calibration can be supplied directly, which would be useful for stable instruments in which the variations in the dispersion are negligible.

3.5 Flux Calibration

When a standard spectrum is wavelength calibrated, it can be compared against literature values to obtain the sensitivity function of the detector. All the standard stars available in IRAF¹⁹ and on the ESO webpage – *Optical and UV Spectrophotometric Standard Stars*²⁰ are available on ASPIRED. See Appendix A for the complete listing of the standard stars and the respective data source. The calibration can be done in either AB magnitude or flux density (per unit wavelength). The two should give similar results, but the response functions found would not be equivalent because fitting to magnitudes is in logarithmic space and smoothing (see below) will have a different effect compared to flux fitting.

Smoothing

A Savitzky-Golay smoothing filter²¹ (Savitzky & Golay 1964, hereafter, SG-filter) can be applied to the data before computing the sensitivity curve. This function works by fitting low-order polynomials to localised subsets of the data to suppress noise in the data at each point interval. It is similar to the commonly used median

¹⁹ <https://github.com/iraf-community/iraf/tree/main/noao/lib/onedstds>

²⁰ <https://www.eso.org/sci/observing/tools/standards/spectra.html>

²¹ https://docs.scipy.org/doc/scipy/reference/generated/scipy.signal.savgol_filter.html

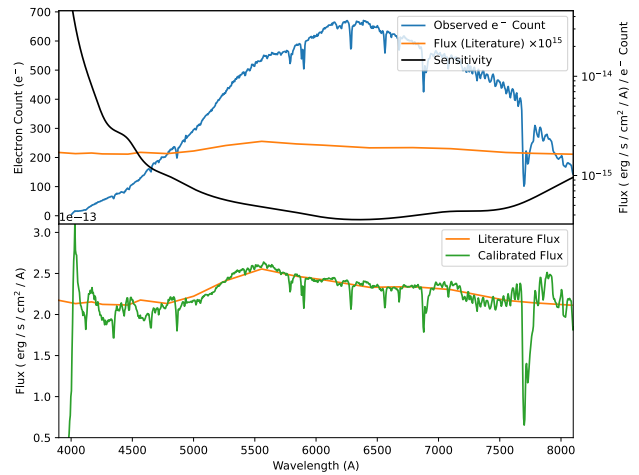


Figure 6. Top: The extracted standard spectrum in electron counts (blue), the literature spectrum in units of flux density (multiplied by 10^{17} ; colour), and the sensitivity function (y-axis on the right; black). Bottom: The literature spectrum (same as the one above) is plotted in orange, and the calibrated observed spectrum is plotted in green.

boxcar filter, but uses more weighted information to better retain information while removing noise. This can be used independently or with continuum fitting (see below), which uses a LOWESS filter. By default, the SG-filter removes only significant noise (e.g. those from unsubtracted cosmic rays).

Continuum Fitting

By default, the continuum of the standard spectrum is found for deriving the sensitivity curve. This process is used after the smoothing procedure (if performed). The continuum is found by fitting the standard spectrum with a LOWESS function as described in Sec. 3.3. This can remove any outlying random noise as well as the absorption lines when computing the sensitivity. Users are reminded to be cautious with this procedure as the removal of the absorption features in computing the sensitivity function can significantly affect the flux calibration near the absorption features.

Sensitivity Curve

The sensitivity curve is computed by dividing the observed standard spectrum by the literature one and then interpolating the result using a spline or a polynomial function (Fig. 6). This can be done with or without any pre-smoothing and/or continuum fitting. Users can also manually supply a sensitivity function as a callable function that accepts a wavelength value and returns the log of the sensitivity value at that wavelength. The sensitivity function does not carry the concept of units; it can be magnitude, flux, or any other appropriate unit (if supplied manually).

3.6 Atmospheric Extinction Correction

ASPIRED currently has four built-in atmospheric extinction curves:

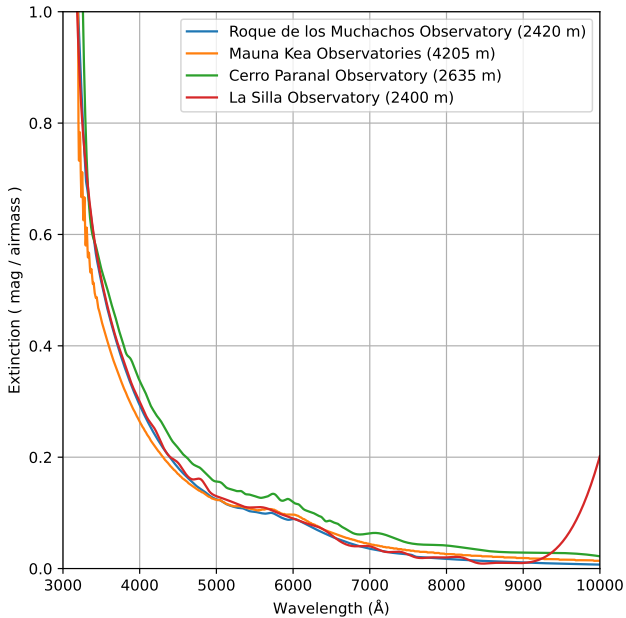


Figure 7. The extinction curves measured at the four sites: Roque de los Muchachos Observatory (2420 m; blue), Mauna Kea Observatories (4205 m; orange), Cerro Paranal Observatory (2635 m; green), and La Silla Observatory (2400 m; red). The extinction table of La Silla Observatory terminates at 9000 Å. The rise at the red end of the curve is an undesired artefact due to extrapolation using a cubic spline. We are explicitly plotting this range to serve as a warning since we opt to preserve the input data as provided.

- (i) Roque de los Muchachos Observatory (2420 m)²²
- (ii) Mauna Kea Observatories (4205 m; Buton et al. 2013)
- (iii) Cerro Paranal Observatory (2635 m; Patat et al. 2011)
- (iv) La Silla Observatory (2400 m)²³

It reports the extinction in magnitude per airmass as a function of wavelength, roughly between 3000 and 10000 Å. Alternatively, a callable function in the appropriate units can be supplied to perform the extinction correction. See Figure 7 for a comparison plot of the atmospheric extinction curves.

3.7 Telluric Absorption Removal

During the process of generating the sensitivity function, masks over the Telluric regions are also used to generate the Telluric absorption profile from the standard star. The default masking regions are 6850 – 6960 and 7580 – 7700 Å only. This profile can then be multiplied by a factor to be determined in order to remove the Telluric absorption features in the science target. The best multiplicative factor is found by minimising the difference between the continuum and the Telluric-absorption-removed-spectrum. An **additional** multiplier can be manually provided to adjust the strength of the subtraction. This is designed for manually fine-tuning the absorption factor; otherwise, it is defaulted to 1.0.

²² http://www.ing.iac.es/astronomy/observing/manuals/ps/tech_notes/tn031.pdf

²³ https://www.eso.org/public/archives/techdocs/pdf/report_0003.pdf

4 DISTRIBUTION

ASPIRED is released under the BSD (3-Clause) License. The source code is hosted on GITHUB, which can be found at <https://github.com/cylamarco/ASPIRED>. The DOI of each version can be found at ZENODO: <https://zenodo.org/record/4463569#.YLjdrKgZyrQ>. For more straightforward installation, ASPIRED is also available at Python Package Index (PyPI): <https://pypi.org/project/aspired> so users can install the software by a simple command of

```
pip install aspired.
```

While the latest stable version can be installed with

```
pip install
git+https://github.com/cylamarco/ASPIRED@main
```

, and the latest development version can be installed with

```
pip install
git+https://github.com/cylamarco/ASPIRED@dev
```

. It is also possible to clone the entire repository and install with the setup script with

```
1 git clone [url to main/dev/a specific commit]
2 python setup.py
```

ACKNOWLEDGEMENTS

This work was partially supported by OPTICON. This project has received funding from the European Union’s Horizon 2020 research and innovation programme under grant agreement No 730890. This material reflects only the authors’ views and the Commission is not liable for any use that may be made of the information contained therein.

This work was partially supported by the Polish NCN grant Daina No. 2017/27/L/ST9/03221.

MCL is supported by a European Research Council (ERC) grant under the European Union’s Horizon 2020 research and innovation program (grant agreement number 852097).

IA is a CIFAR Azrieli Global Scholar in the Gravity and the Extreme Universe Program and acknowledges support from that program, from the ERC under the European Union’s Horizon 2020 research and innovation program (grant agreement number 852097), from the Israel Science Foundation (grant number 2752/19), from the United States - Israel Binational Science Foundation (BSF), and from the Israeli Council for Higher Education Alon Fellowship.

The LT is operated on the island of La Palma by Liverpool John Moores University in the Spanish Observatorio del Roque de los Muchachos of the Instituto de Astrofísica de Canarias with financial support from the UK Science and Technology Facilities Council.

This work makes use of observations from the Las Cumbres Observatory global telescope network. We have made use of the data collected from the FLOYDS spectrograph on the LCOGT 2m telescope at both Siding Spring, Australia and Maui, HI, United States.

REFERENCES

- Astropy Collaboration et al., 2013, *A&A*, **558**, A33
- Astropy Collaboration et al., 2018, *AJ*, **156**, 123
- Bohlin R. C., 1996, *AJ*, **111**, 1743

- Bohlin R. C., Colina L., Finley D. S., 1995, *AJ*, **110**, 1316
- Brown T. M., et al., 2013, *PASP*, **125**, 1031
- Buton C., et al., 2013, *A&A*, **549**, A8
- Carnall A. C., 2017, arXiv e-prints, p. arXiv:1705.05165
- Cepa J., et al., 2000, in Iye M., Moorwood A. F., eds, Society of Photo-Optical Instrumentation Engineers (SPIE) Conference Series Vol. 4008, Optical and IR Telescope Instrumentation and Detectors. pp 623–631, doi:10.1117/12.395520
- Cleveland W. S., 1979, *Journal of the American Statistical Association*, **74**, 829
- Craig M., et al., 2017, astropy/ccdproc: v1.3.0.post1, doi:10.5281/zenodo.1069648, <https://doi.org/10.5281/zenodo.1069648>
- Dalcin L. D., Paz R. R., Kler P. A., Cosimo A., 2011, *Advances in Water Resources*, **34**, 1124
- Eggen O. J., Greenstein J. L., 1965, *ApJ*, **141**, 83
- Filippenko A., Greenstein J. L., 1984, *PASP*, **96**, 530
- Fischler M., Bolles R., 1981, *Communications of the ACM*, **24**, 381
- Hamuy M., Walker A. R., Suntzeff N. B., Gigoux P., Heathcote S. R., Phillips M. M., 1992, *PASP*, **104**, 533
- Hamuy M., Suntzeff N. B., Heathcote S. R., Walker A. R., Gigoux P., Phillips M. M., 1994, *PASP*, **106**, 566
- Harris C. R., et al., 2020, *Nature*, **585**, 357–362
- Hook I. M., Jørgensen I., Allington-Smith J. R., Davies R. L., Metcalfe N., Murowinski R. G., Crampton D., 2004, *PASP*, **116**, 425
- Horne K., 1986, *PASP*, **98**, 609
- Kausch W., et al., 2015, *A&A*, **576**, A78
- Krekel H., Oliveira B., Pfanschmidt R., Bruynooghe F., Laughner B., Bruhin F., 2004, pytest 6.2, <https://github.com/pytest-dev/pytest>
- Lam M. C., 2021, cyllamarco/ASPIRED: Initial Development Release v0.3.1, doi:10.5281/zenodo.4463569, <https://doi.org/10.5281/zenodo.4463569>
- Lam M. C., Smith R. J., Veitch-Michaelis J., Steele I. A., McWhirter P. R., 2020a, arXiv e-prints, p. arXiv:2012.03505
- Lam M. C., Hambly N. C., Lodieu N., Blouin S., Harvey E. J., Smith R. J., Gálvez-Ortiz M. C., Zhang Z. H., 2020b, *MNRAS*, **493**, 6001
- Mandel E., Vikhlinin A., 2021, ericmandel/js9, doi:10.5281/zenodo.596052, <https://doi.org/10.5281/zenodo.596052>
- Marsh T. R., 1989, *PASP*, **101**, 1032
- Massey P., Strobel K., Barnes J. V., Anderson E., 1988, *ApJ*, **328**, 315
- McCully C., et al., 2018, astropy/astroscrappy: v1.0.5 Zenodo Release, doi:10.5281/zenodo.1482019, <https://doi.org/10.5281/zenodo.1482019>
- Moehler S., et al., 2014a, *The Messenger*, **158**, 16
- Moehler S., et al., 2014b, *A&A*, **568**, A9
- Noll S., Kausch W., Kimeswenger S., Barden M., Jones A. M., Modigliani A., Szyszka C., Taylor J., 2014, *A&A*, **567**, A25
- Oke J. B., 1990, *AJ*, **99**, 1621
- Patat F., et al., 2011, *A&A*, **527**, A91
- Piascik A. S., Steele I. A., Bates S. D., Mottram C. J., Smith R. J., Barnsley R. M., Bolton B., 2014, in Proc. SPIE. p. 91478H, doi:10.1117/12.2055117
- Piskunov N., Wehrhahn A., Marquart T., 2021, *A&A*, **646**, A32
- Plotly Technologies Inc. 2015, Collaborative data science, <https://plot.ly>
- Prochaska J. X., et al., 2020a, pypeit/PypeIt: Release 1.0.0, doi:10.5281/zenodo.3743493
- Prochaska J. X., et al., 2020b, *Journal of Open Source Software*, **5**, 2308
- Savitzky A., Golay M. J. E., 1964, *Analytical Chemistry*, **36**, 1627
- Seabold S., Perktold J., 2010, in 9th Python in Science Conference.
- Smette A., et al., 2015, *A&A*, **576**, A77
- Song Q., Zhang T., Wang Z., Zhang S., Yang L., 2018, *Appl. Opt.*, **57**, 6876
- Stone R. P. S., 1977, *ApJ*, **218**, 767
- Tody D., 1986, in Crawford D. L., ed., Society of Photo-Optical Instrumentation Engineers (SPIE) Conference Series Vol. 627, Instrumentation in astronomy VI. p. 733, doi:10.1117/12.968154
- Tody D., 1993, in Hanisch R. J., Brissenden R. J. V., Barnes J., eds, Astronomical Society of the Pacific Conference Series Vol. 52, Astronomical Data Analysis Software and Systems II. p. 173
- Veitch-Michaelis J., Lam M. C., 2020a, in Zenodo Software package. p. 17517, doi:10.5281/zenodo.4117517
- Veitch-Michaelis J., Lam M. C., 2020b, in Pizzo R., Deul E. R., Mol J. D., de Plaa J., Verkouter H., eds, Astronomical Society of the Pacific Conference Series Vol. 527, Astronomical Society of the Pacific Conference Series. p. 627 (arXiv:1912.05883)
- Virtanen P., et al., 2020, *Nature Methods*, **17**, 261
- Zechmeister M., Anglada-Escudé G., Reiners A., 2014, *A&A*, **561**, A59
- van Dokkum P. G., 2001, *PASP*, **113**, 1420

APPENDIX A: STANDARD STARS

We provide the list of standard stars available from the ESO, ING and iraf catalogues (see links in the respective group for the file source). We call the name of the set of data a *library*; the naming is self-explanatory:

```
library_list = [
    'esoctiostan', 'esohststan', 'esookestan',
    'esowdstan', 'esoxshooter', 'ing_oke',
    'ing_sto', 'ing_og', 'ing_mas', 'ing_fg',
    'irafblackbody', 'irafbstdscal', 'irafctiocal',
    'irafctionewcal', 'irafiidscal', 'irafirscal',
    'irafoke1990', 'irafredcal', 'irafspec16cal',
    'irafspec50cal', 'irafspechayescal'
]
```

The following lists all the available stars in each of the libraries. In iraf, a number of stars with multiple commonly used designations are run through a name-resolver. We do not provide such utility. We adopt the name from the filenames as they are.

A1 European Southern Observatory (ESO)

ESO Hamuy et al. (1992, 1994) Standards²⁴

```
esoctiostan = [
    'cd32d9927', 'cd_34d241', 'eg21', 'eg274',
    'feige110', 'feige56', 'hilt600', 'hr1544',
    'hr3454', 'hr4468', 'hr4963', 'hr5501',
    'hr718', 'hr7596', 'hr7950', 'hr8634',
    'hr9087', 'ltt1020', 'ltt1788', 'ltt2415',
    'ltt3218', 'ltt3864', 'ltt4364', 'ltt4816',
    'ltt6248', 'ltt7379', 'ltt745', 'ltt7987',
    'ltt9239', 'ltt9491'
]
```

ESO Bohlin et al. (1995); Bohlin (1996) HST Standards²⁵

```
esohststan = [
    'agk81d266', 'bd28d4211', 'bd33d2642',
    'bd75d325', 'bpm16274', 'feige110',
    'feige34', 'g191b2b', 'g93_48', 'gd108',
    'gd50', 'grw70d5824', 'hd49798', 'hd60753',
    'hd93521', 'hr153', 'hr1996', 'hr4554',

```

²⁴ <https://www.eso.org/sci/observing/tools/standards/spectra/hamuystandards.html>

²⁵ <https://www.eso.org/sci/observing/tools/standards/spectra/hststandards.html>

```
'hr5191', 'hr7001', 'hz2', 'hz21', 'hz4',
'hz44', 'lb227', 'lds749b', 'ngc7293'
```

ESO Oke (1990) Standard ²⁶

```
esookestan = [
'bd25d4655', 'bd28d4211', 'bd33d2642',
'bd75d325', 'feige110', 'feige34',
'feige66', 'feige67', 'g138_31',
'g158_100', 'g191b2b', 'g193_74', 'g24_9',
'g60_54', 'gd108', 'gd248', 'gd50',
'grw70d5824', 'hd93521', 'hz21', 'hz4',
'hz44', 'ltt9491', 'ngc7293', 'sa95_42'
```

ESO Bohlin et al. (1995) WD Standards ²⁷

```
esowdstan = [
'agk_81d266_005', 'alpha_lyr_004',
'bd_25d4655_002', 'bd_28d4211_005',
'bd_33d2642_004', 'bd_75d325_005',
'feige110_005', 'feige34_005',
'feige66_002', 'feige67_002',
'g93_48_004', 'gd108_005', 'gd50_004',
'gd71', 'grw_70d5824_005', 'hd93521_005',
'hz21_005', 'hz2_005', 'hz44_005',
'hz4_004', 'lb227_004', 'lds749b_005',
'ltt9491_002', 'ngc7293_005'
```

ESO X-shooter Standards (Moehler et al. 2014a,b) ²⁸

```
esoxshooter = [
'EG274', 'Feige110', 'GD153', 'GD71',
'LTT3218', 'LTT7987'
```

A2 Issac Newton Group of Telescopes (ING)

The ING listing is grouped into five sets by the last name of the authors²⁹.

Oke (1990) Standards

```
ing_oke = [
'bd254', 'bd28', 'bd33', 'bd75', 'erib',
'f110', 'f24', 'f34', 'f66', 'f67',
'g138', 'g158', 'g191new', 'g191old',
'g193', 'g24', 'g47', 'g60', 'g99',
'gd108', 'gd140', 'gd190', 'gd248',
'gd50', 'grw705new', 'grw705old',
```

²⁶ https://www.eso.org/sci/observing/tools/standards/spectra/okestandards_rev.html

²⁷ <https://www.eso.org/sci/observing/tools/standards/spectra/wdstandards.html>

²⁸ <https://www.eso.org/sci/observing/tools/standards/spectra/Xshooterspec.html>

²⁹ http://www.ing.iac.es/Astronomy/observing/manuals/html_manuals/tech_notes/tn065-100/workflux.html

```
'grw708', 'grw73', 'hd935', 'he3',
'hz14', 'hz2', 'hz21', 'hz29', 'hz43',
'hz44new', 'hz44old', 'hz4new', 'hz4old',
'hz7', 'l1363', 'l1512', 'l745', 'l870',
'l930', 'l970', 'lb1240', 'lb227',
'lds235', 'lds749', 'ltt', 'ngc', 'r627',
'r640', 'sa29', 'sa95', 't573', 'w1346',
'w485'
```

Stone (1977) Standards

```
ing_sto = [
'bd08', 'bd253', 'bd28', 'bd33', 'bd40',
'f110', 'f15', 'f25', 'f34', 'f56', 'f92',
'f98', 'h102', 'h600', 'hz15', 'k27'
```

Eggen & Greenstein (1965) Standards

```
ing_og = ['bd17', 'bd26', 'hd194', 'hd849']
```

Massey et al. (1988) Standards

```
ing_mas = [
'bd28', 'cyg', 'eg81', 'f110', 'f34', 'f66',
'f67', 'g191', 'gd140', 'h600', 'hd192',
'hd217', 'hz14', 'hz44', 'pg0205', 'pg0216',
'pg0310', 'pg0823', 'pg0846', 'pg0934',
'pg0939', 'pg1121', 'pg1545', 'pg1708',
'w1346'
```

Filippenko & Greenstein (1984) Standards

```
ing_fg = ['g138', 'g158', 'g24', 'gd248']
```

A3 iraf Standards

The complete list of iraf standards are available at ³⁰.

```
irafblackbody = [
'U', 'B', 'V', 'R', 'I', 'J', 'H', 'K', 'L',
'Lprime', 'M'
```

```
irafbstdscal = [
'hr718', 'hr3454', 'hr3982', 'hr4468',
'hr4534', 'hr5191', 'hr5511', 'hr7001',
'hr7596', 'hr7950', 'hr8634', 'hr9087',
'hr15318', 'hr74280', 'hr100889',
'hr188350', 'hr198001', 'hr214923',
'hr224926'
```

```
irafctiocal = [
'bd8', 'bd25', 'bd73632', 'cd32', 'eg11',
'eg21', 'eg26', 'eg31', 'eg54', 'eg63',
'eg76', 'eg79', 'eg99', 'eg139', 'eg149',
```

³⁰ <https://github.com/iraf-community/iraf/tree/main/noao/lib/onedstds>

```

'eg158', 'eg248', 'eg274', 'f15', 'f25',
'f56', 'f98', 'f110', 'feige15', 'feige25',
'feige56', 'feige98', 'feige110', 'g2631',
'g9937', 'g16350', 'h600', 'hz2', 'hz4',
'hz15', 'kopf27', 'l377', 'l1020', 'l1788',
'l2415', 'l2511', 'l3218', 'l3864', 'l4364',
'l4816', 'l6248', 'l7379', 'l7987', 'l8702',
'l9239', 'l9491', 'l74546', 'l93080',
'l97030', 'lds235', 'lds749', 'ltt4099',
'ltt8702', 'rose627', 'w1346', 'w485a',
'wolf1346', 'wolf485a'
]
irafactionewcal = [
'cd32', 'eg21', 'eg274', 'f56', 'f110',
'h600', 'l377', 'l745', 'l1020', 'l1788',
'l2415', 'l2511', 'l3218', 'l3864', 'l4364',
'l4816', 'l6248', 'l7379', 'l7987', 'l9239',
'l9491', 'cd32blue', 'eg21blue', 'eg274blue',
'f56blue', 'f110blue', 'h600blue', 'l377blue',
'l1020blue', 'l1788blue', 'l2415blue',
'l2511blue', 'l3218blue', 'l3864blue',
'l4364blue', 'l4816blue', 'l6248blue',
'l7379blue', 'l7987blue', 'l9239blue',
'l9491blue', 'cd32red', 'eg21red', 'eg274red',
'f56red', 'f110red', 'h600red', 'l377red',
'l745red', 'l1020red', 'l1788red', 'l2415red',
'l2511red', 'l3218red', 'l3864red', 'l4364red',
'l4816red', 'l6248red', 'l7379red', 'l7987red',
'l9239red', 'l9491red'
]
irafiidscal = [
'40erib', 'amcvn', 'bd7781', 'bd73632',
'bd82015', 'bd253941', 'bd284211', 'bd332642',
'bd404032', 'eg11', 'eg20', 'eg26', 'eg28',
'eg29', 'eg31', 'eg33', 'eg39', 'eg42',
'eg50', 'eg54', 'eg63', 'eg67', 'eg71',
'eg76', 'eg77', 'eg79', 'eg91', 'eg98',
'eg99', 'eg102', 'eg119', 'eg129', 'eg139',
'eg144', 'eg145', 'eg148', 'eg149', 'eg158',
'eg162', 'eg182', 'eg184', 'eg193', 'eg247',
'eg248', 'feige15', 'feige24', 'feige25',
'feige34', 'feige56', 'feige92', 'feige98',
'feige110', 'g88', 'g2610', 'g2631', 'g4718',
'g9937', 'g12627', 'g14563', 'g16350',
'g191b2b', 'gd128', 'gd140', 'gd190',
'gh7112', 'grw705824', 'grw708247',
grw738031', 'he3', 'hz2', 'hz4', 'hz7',
'hz14', 'hz15', 'hz29', 'hz43', 'hz44',
'kopf27', 'hiltner102', 'hiltner600',
'l8702', 'l13633', 'l14094', 'l74546a',
'l93080', 'l97030', 'l140349', 'l151234b',
'lft1655', 'lb227', 'lb1240', 'lds235b',
'lds749b', 'lp414101', 'ltt4099', 'ltt8702',
'ltt13002', 'ltt16294', 'ross627', 'ross640',
'sa29130', 'sao131065', 'ton573', 'wolf1346',
'wolf485a'
]
irafirscal = [
'bd082015', 'bd174708', 'bd253941', 'bd262606',
'bd284211', 'bd332642', 'bd404032', 'eg50',
'eg71', 'eg139', 'eg158', 'eg247', 'feige15',
'feige25', 'feige34', 'feige56', 'feige92',
'feige98', 'feige110', 'g191b2b', 'hd2857',
'hd17520', 'hd19445', 'hd60778', 'hd74721',
'hd84937', 'hd86986', 'hd109995', 'hd117880',
'hd161817', 'hd192281', 'hd217086', 'he3',
'hiltner102', 'hiltner600', 'hr7001', 'hz44',
'kopf27', 'wolf1346'
]
irafoke1990 = [
'bd75325', 'bd284211', 'feige34', 'feige67',
'feige110', 'g249', 'g13831', 'g191b2b',
'g19374', 'gd108', 'gd248', 'hz21', 'ltt9491',
'eg71', 'eg158', 'eg247'
]
irafredcal = [
'40erib', 'amcvn', 'bd7781', 'bd73632',
'bd174708', 'bd262606', 'eg20', 'eg33',
'eg50', 'eg54', 'eg63', 'eg67', 'eg76',
'eg79', 'eg91', 'eg98', 'eg99', 'eg102',
'eg119', 'eg129', 'eg139', 'eg144', 'eg145',
'eg148', 'eg149', 'eg158', 'eg162', 'eg182',
'eg184', 'eg193', 'eg247', 'eg248',
'feige24', 'g2610', 'g2631', 'g4718',
'g9937', 'g12627', 'g14563', 'g16350',
'g191b2b', 'gd140', 'gd190', 'grw705824',
'grw708247', 'grw738031', 'hd19445',
'hd84937', 'he3', 'hz29', 'hz43', 'hz44',
'l13633', 'l14094', 'l151234b', 'l74546a',
'l93080', 'l97030', 'lds235b', 'lds749b',
'lft1655', 'ltt4099', 'ltt8702', 'ltt16294',
'ross627', 'ross640', 'sa29130',
'sao131065', 'wolf1346', 'wolf485a'
]
irafspec16cal = [
'hd15318', 'hd30739', 'hd74280', 'hd100889',
'hd114330', 'hd129956', 'hd188350',
'hd198001', 'hd214923', 'hd224926', 'hr718',
'hr1544', 'hr3454', 'hr4468', 'hr4963',
'hr5501', 'hr7596', 'hr7950', 'hr8634',
'hr9087', 'hd15318blue', 'hd30739blue',
'hd74280blue', 'hd100889blue', 'hd114330blue',
'hd129956blue', 'hd188350blue', 'hd198001blue',
'hd214923blue', 'hd224926blue', 'hr718blue',
'hr1544blue', 'hr3454blue', 'hr4468blue',
'hr4963blue', 'hr5501blue', 'hr7596blue',
'hr7950blue', 'hr8634blue', 'hr9087blue',
'hd15318red', 'hd30739red', 'hd74280red',
'hd100889red', 'hd114330red', 'hd129956red',
'hd188350red', 'hd198001red', 'hd214923red',
'hd224926red', 'hr718red', 'hr1544red',
'hr3454red', 'hr4468red', 'hr4963red',
'hr5501red', 'hr7596red', 'hr7950red',
'hr8634red', 'hr9087red'
]
irafspec50cal = [
'bd284211', 'cygob2no9', 'eg20', 'eg42',
'eg71', 'eg81', 'eg139', 'eg158', 'eg247',
'feige34', 'feige66', 'feige67', 'feige110',
'g191b2b', 'gd140', 'hd192281', 'hd217086',

```

```
'hilt600', 'hz14', 'hz44', 'pg0205134',  
'pg0216032', 'pg0310149', 'pg0823546',  
'pg0846249', 'pg0934554', 'pg0939262',  
'pg1121145', 'pg1545035', 'pg1708602',  
'wolf1346'  
]  
irafspechayescal = [  
'bd284211', 'cygob2no9', 'eg42', 'eg71',  
'eg81', 'eg139', 'eg158', 'eg247', 'feige34',  
'feige66', 'feige67', 'feige110', 'g191b2b',  
'gd140', 'hd192281', 'hd217086', 'hilt600',  
'hz14', 'hz44', 'pg0205134', 'pg0216032',  
'pg0310149', 'pg0823546', 'pg0846249',  
'pg0934554', 'pg0939262', 'pg1121145',  
'pg1545035', 'pg1708602', 'wolf1346'  
]
```

This paper has been typeset from a \TeX/L\AA\TeX file prepared by the author.